Chalcogenide Letters Vol. 17, No. 1, January 2020, p. 25 - 31

SUPERIMPOSED EQUALLY ORIENTED DIFFRACTION GRATINGS FORMED IN As_2S_3 FILMS

S. A. SERGEEV*, M. S. IOVU, A. YU MESHALKIN
Institute of Applied Physics, Chisinau, Republic of Moldova

Surface relief diffraction structures composed of two or three superimposed unidirectional gratings with unequal grating periods were produced using the electron beam recording and subsequent chemical etching. Diffraction patterns produced by different diffraction structures were studied. In addition to the main diffracted beams the low-intensity "ghost" diffracted beams were created by some grating structures. Their appearance was caused by a difference in spatial frequency between gratings and by summation of spatial frequencies as well. The calculated grating periods corresponding to "ghost" diffracted beams were found to agree well with those determined from diffraction patterns.

(Received September 30, 2019; Accepted January 9, 2020)

Keywords: Superimposed gratings, Diffraction pattern, Diffraction efficiency, Beat period, "Ghost" beam.

1. Introduction

Up to the present, amorphous chalcogenide thin films have been promising materials for optical and electron beam recording of diffractive optical elements due to their advanced properties. Both the refractive index and surface relief gratings can be produced in these materials via structural changes in amorphous films induced by irradiation. The first studies [1, 2] showed that electron beam irradiation results in an increase in the refractive index of chalcogenide films. From a study of index gratings with a period of 2 μm, it was found [2] that a single grating line formed by electron beam irradiation has a Gaussian profile. The nonsinusoidal grating of period Λ was considered from Fourier analysis as composed of sinusoidal gratings of different periods Λ/k, where k=1, 2, 3,... [2]. The dose dependence of the refraction index increment $\Delta n\ (q)$ in As_2S_3 was presented in [3]. According to this curve, Δn is approximately proportional to the 0.79th power of q in the $\Delta n < 0.05$ region. A maximum value Δn of about 0.06 was obtained for grating. It is concluded in [4] that, for the investigated As_xS_{100-x} compositions (x=30÷45), the stoichiometric As_2S_3 composition has the largest change in the refractive index (~0.08) induced by electron-beam irradiation.

The development of computer-controlled electron beam recording has significantly extended the use of the latter for producing of different integrated optics components, many of which were reviewed in [5]. Owing to a large index increment, thin graded-index Fresnel lenses were fabricated in As_2S_3 films [4]. The nano-structures were fabricated in chalcogenide films using electron-beam lithography [6,7]. The gratings formed in arsenic sulfide films [7] have lines with widths of 27 nm, a separation of 7 nm, and heights from 80 to 250 nm. Grayscale electron-beam lithography in chalcogenide films was developed, and ultrathin Fresnel lenses were fabricated in the Ag/As_2S_3 layer using this technique [8]. Electron-beam irradiation causes surface modulation in nanomultilayer structures based on chalcogenide glasses. Because of this, the surface relief patterns composed of pixels with a height of about 200 nm were formed in $Ge_5As_{37}S_{58}$–Se nanomultilayer structures by direct electron-beam recording [9].

Owing to a wide dose range of the index increment Δn, the chalcogenide films are promising materials for producing complicated diffraction structures. We used the electron beam recording to fabricate grating structures composed of superimposed gratings. A grating structure composed of six equally spaced in orientation index gratings without any influence of

* Corresponding author: sersegal@mail.ru

superimposition on their diffraction efficiencies was formed in As_2S_3 films [10]. Superimposed gratings can be used in some fields of optoelectronics. For example, a multibeam light diffraction created by structures composed of several superimposed gratings with rectangular profiles was used [11] for optical coding. A set of surface relief grating structures composed of unidirectional superimposed gratings was formed in As_2S_3 films by electron beam recording and the consequence wet etching. The features of diffraction patterns created by such grating structures are reported in the present paper.

2. Experimental

Amorphous As_2S_3 films with a thickness of about 1.5 μm were thermally deposited in vacuum on glass substrates with the underlying semitransparent electrode. Electron-beam recording of grating structures was performed using the scanning electron microscope (SEM) BS 300 (Tesla). Two or three superimposed unidirectional gratings were consecutively recorded using the SEM raster system. Grating periods varied from 0.8 to 4.0 μm. Their values were determined from diffracted patterns. A different order of recording of superimposed gratings was used. The dose of electron irradiation was determined by the electron beam current (I) and was calculated from the formula [12]

$$q = \frac{I \cdot \tau}{l \cdot d} \quad , \tag{1}$$

where τ is a scan time of one line, l is a length of the line, and d is an electron beam diameter. An acceleration voltage of 23 kV was used. The relief grating structures were prepared by chemical etching in the water solution of KOH. A short etching procedure (about 5 s) was used for the surface relief modulation of As_2S_3 film The first-order diffraction efficiencies of the superimposed gratings were measured in transmission mode at normal incidence of a laser beam (0.633 μm) and calculated as a ratio of light intensities of diffracted and incident laser beams. The diffraction patterns presented below were created under the above-mentioned conditions. The first-, second-, and third- order diffracted spots are marked as m_i=1, m_i=2, and m_i=3 respectively, where i = 1, 2, 3 corresponds to the e-beam recorded grating with a grating period Λ_i.

3. Results

The AFM (Atomic Force Microscope) image of a surface relief diffraction structure composed of two gratings with grating periods Λ_1=1.0 μm and Λ_2=0.9 μm formed in the AsS film is shown in Fig. 1.

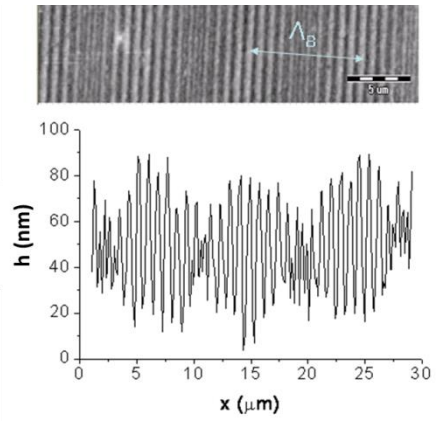

Fig. 1. AFM image of the surface relief grating structure composed of superimposed gratings with Λ_1=1.0 μm and Λ_2=0.9 μm formed in AsS film and a grating structure profile. Λ_B is a beat period.

Superimposition of two straight-line gratings with unequal grating periods Λ_1 and Λ_2 forms a Moiré pattern on the surface relief structure. Its formation is caused by a total spatial distribution of the etching velocity of a chalcogenide film, which in turn is modulated during the recording of a grating structure by superimposition of electron-beam irradiations with a different periodicity.

The strong lines overlapping resulted in a high depth of surface modulation (Δh) of 70-80 nm. In regions of the weak lines overlapping, the Δh value of about 15-20 nm was estimated. Periodically varied level of lines overlapping causes a periodic modulation of the surface relief depth. The period of the Moiré pattern of the grating structure composed of two straight-line superimposed gratings is equal to a beat period (Λ_B) between gratings

Fig. 2. Diffraction pattern from a structure composed of superimposed gratings with Λ_1=1 μm and Λ_2=0.92 μm formed in As_2S_3 film

$$\Lambda_B = \frac{\Lambda_1 \cdot \Lambda_2}{|\Lambda_1 - \Lambda_2|} \tag{2}$$

This formula is derived from the difference in spatial frequency between two superimposed gratings. For the structure shown in Fig. 1, the beat period is Λ_B = 9.0 μm.

A similar grating structure was formed in the As_2S_3 film. The diffraction pattern produced by this grating structure is shown in Fig. 2.

There are two distinct first-order diffraction spots (m_1=1 and m_2=1) in the diffraction pattern. The periodicity Λ_B results in the formation of the additional diffraction grating that produces low-intensity diffracted laser beams, so-called "ghost" beams. Corresponding "ghost" diffracted spots are located near a zero-order spot in the diffraction pattern, where they are marked by m_{1G}. Grating periods Λ_1 and Λ_2 of about 0.92 μm and 1.0 μm, respectively, were calculated from the diffraction pattern. Thus, the grating periods differ only by about 80 nm. The beat period Λ_B of about 12 μm was determined as well. The corresponding diffracted beam has a diffraction angle of about 3°. The Λ_B value of 11.5 μm calculated from (2) is in good agreement with the one determined experimentally.

A more complicated diffraction pattern was formed by a grating structure composed of superimposed gratings with Λ_1=2.0 μm and Λ_2=0.92 μm (Fig. 3). This structure produced three "ghost" spots. The spot marked as m_{3G}=1 was created by the beat period Λ_{B3} between gratings with Λ_1 and Λ_2 periods.

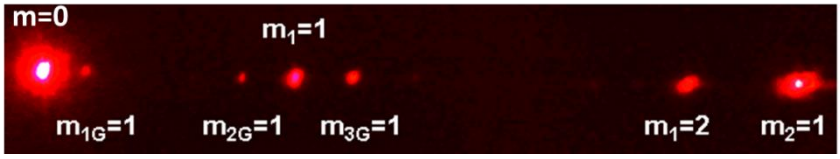

Fig. 3. Diffraction pattern from a structure composed of superimposed gratings with Λ_1=2.0 μm and Λ_2=0.92 μm formed in As_2S_3 film.

According to [2], the nonsinusoidal grating is composed of a set of sinusoidal gratings. With this taken into account, the subgrating with a grating period $\Lambda_1/2$ can be considered as well. The spot m_{1G}=1 is created by the beat period Λ_{B1} between a grating with Λ_2 and subgrating with

$\Lambda_1/2$. Similarly, the spot $m_{2G}=1$ is created by the beat period Λ_{B2} between the subgrating with a period $\Lambda_1/2$ and a grating with Λ_{B3}. Comparison of the beat periods calculated from (2) with those determined experimentally is presented in Table 1.

Table 1. Calculated and experimentally determined beat periods.

Λ_1 (μm)	Λ_2 (μm)	Λ_{B1} (μm)		Λ_{B2} (μm)		Λ_{B3} (μm)	
exp.	exp.	exp.	calc.	exp.	calc.	exp.	calc.
2.00	0.915	10.42	10.65	2.475	2.466	1.678	1.685

Good agreement between the calculated and experimentally determined beat periods supports the model of calculation.

The diffraction pattern from a grating structure composed of three superimposed gratings with Λ_1=0.9 μm, Λ_2=1.0 μm, and Λ_3=1.1 μm is shown in Fig. 4. There are three distinct first-order diffracted spots in the diffraction pattern.

Fig. 4. Diffraction pattern from a structure composed of superimposed gratings with Λ_1=1.1 μm, Λ_2=1 μm and Λ_3=0.9 μm formed in As_2S_3 film

The influence of the conditions of recording on the efficiency of these superimposed gratings is presented in Fig. 5. Different orders of the recording of superimposed gratings are shown by arrows in Fig. 5. Open symbols in the dose dependences indicate primarily recording of grating with Λ_1=0.9 μm, and full symbols correspond to the primary recording of a grating with Λ_1=1.1 μm. As is seen, the latter case of recording yields a higher efficiency for each superimposed grating. The optimal dose of electron irradiation of about 0.8 mC·cm^{-2} was determined from dose dependences of the diffraction efficiency.

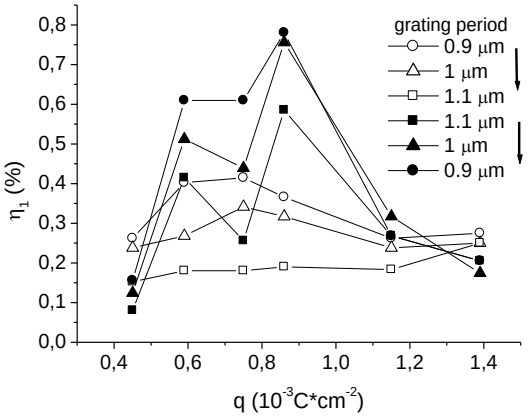

Fig. 5. Dose dependences of the diffraction efficiency of superimposed gratings with Λ_1=1.1 μm, Λ_2=1.0 μm and Λ_3=0.9 μm for different orders (open and full symbols) of recording of gratings (shown by arrows).

The diffraction structure composed of superimposed gratings with Λ_1=2.0 μm, Λ_2=1.9 μm, and Λ_3=1.8 μm was recorded with a dose irradiation of 0.6 mC·cm^{-2}. No influence of the order of recording of gratings on their diffraction efficiencies was observed in this case. The diffraction pattern from this grating structure is shown in Fig. 6.

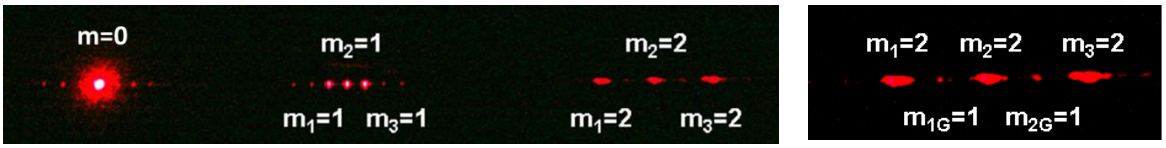

a) *b)*

Fig. 6. (a) Diffraction pattern from a structure composed of superimposed gratings with Λ_1=2.0 μm, Λ_2=1.9 μm and Λ_3=1.8 μm and (b) a fragment of the pattern with second order diffracted spots

First-order diffracted beams produced by this diffraction structure have rather close angles of diffraction. Particularly, the difference between diffraction angles of beams produced by gratings with Λ_2=1.9 μm and Λ_3=2.0 μm is about 1º. Three distinct first-order diffracted spots are seen in this case (Fig. 6a). Between the second-order diffraction spots, there are additional spots of weak intensity (Fig. 6b). The formation of the corresponding "ghost" diffracted beams is caused by the summation of two different spatial frequencies. The positions of such "ghost" beams were determined using a Fast Fourier Transform (FTT) simulation of the diffraction pattern from superimposed gratings [11]. According to [11], the corresponding grating period formed by the summation of two gratings with grating periods Λ_1 and Λ_2 can be calculated by formula

$$\Lambda_S = \frac{\Lambda_1 \cdot \Lambda_2}{\Lambda_1 + \Lambda_2} \tag{3}$$

This formula corresponds to summation of the spatial frequencies of the superimposed gratings. In the case of close Λ_1 and Λ_2 values, Λ_S can also be calculated with high accuracy from the empirical formula $\Lambda_S=(\Lambda_1+\Lambda_2)/4$. The calculated Λ_S values for the pairs of periods (Λ_1,Λ_2), (Λ_2,Λ_3), and (Λ_1,Λ_3) are 0.924, 0.974, and 0.947 μm, respectively. Note that, in the latter case, the propagation direction of the corresponding "ghost" beam almost coincides with that of the second-order diffracted beam from a grating with Λ_2=1.9 μm.

The diffraction pattern created by superimposed gratings with periods Λ_1, Λ_2, and Λ_3 of about 3.5, 2.1, and 0.96 μm, respectively, is shown in Fig. 7.

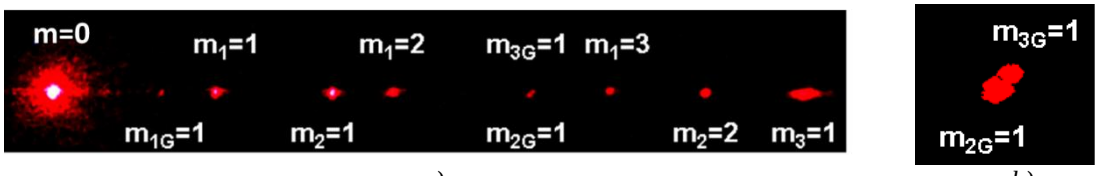

a) *b)*

Fig. 7. (a) Diffraction pattern from grating structure composed of superimposed gratings with Λ_1=3.5 μm, Λ_2=2.1 μm and Λ_3=0.96 μm and (b) a fragment of the pattern with closely located "ghost" diffracted spots

Magnification of the pattern fragment (Fig. 7b) allowed us to reveal a pair of "ghost" diffracted spots located side by side between second-order diffracted spots m_1=2 and m_2=2. The "ghost" spot marked as m_{2G}=1 is created by a beat period Λ_{B2} formed by the superimposition of the gratings with Λ_1 and Λ_3. The "ghost" spot m_{3G}=1 is created by period Λ_{S1}, which results from the summation of the spatial frequencies of gratings with Λ_1 and Λ_2. The "ghost" spot m_{1G}=1 is created by a beat period Λ_{B1}, which is also formed by the superimposition of the gratings with Λ_1 and Λ_2.

The period values Λ_{B1}, Λ_{B2} , and Λ_{S1} calculated from (2) and (3) and those determined experimentally are presented in Table 2.

Table 2. Calculated and experimentally determined period values Λ_{B1}, Λ_{B2} and Λ_{S1}

Λ_1 (μm)	Λ_2 (μm)	Λ_3 (μm)	Λ_{B1} (μm)		Λ_{B2} (μm)		Λ_{S1} (μm)	
exp.	exp.	exp.	calc.	exper.	calc.	exp.	calc.	exp.
3.476	2.092	0.963	5.254	5.240	1.332	1.323	1.306	1.308

Once again, good agreement of the calculated period values with those experimentally determined supports the model of calculation we have used. Thus, two different "ghost" diffracted beams were created by the pair of gratings with periods Λ_1 and Λ_2. A similar pair of the "ghost" beams was observed in [11].

4. Discussions

Electron beam irradiation causes structural changes in the chalcogenide film, which in turn result in a modulation of its refractive index and the rate of chemical dissolution. During the consecutive recording of several superimposed unidirectional gratings, the summation of electron irradiation profiles occurs. This can distort profiles of each superimposed grating. Recording of the complicated grating structures in As_2S_3 film is possible due to the accumulation of changes in its properties under repeated electron irradiation. This yields a correlation of the surface modulation profile in the film with a spatial distribution of the absorbed energy of electrons. As a result, the total surface relief profile of the grating structure formed under appropriate conditions includes profiles of the recorded superimposed gratings. The interaction of a readout laser beam with such a grating structure creates diffracted beams from each recorded grating. The high dose of irradiation may cause a significant distortion of the grating structure profile due to the lateral widening of regions of induced changes in film properties. This applies particularly to recording of the grating structures with submicron and nano-sized features. The group of superimposed gratings with grating periods of 1.1 μm, 1.0 μm, and 0.9 μm is just such a structure, and an optimal irradiation dose for its recording was determined. The influence of the order of recording of gratings on grating efficiencies is not yet clear. It seems that the overlapping of exposed film parts during the recording of grating lines should be taken into account. Such areas are less overlapped when the line spacing is 1.1 μm than those with a line spacing of 0.9 μm. Because of this, the smaller the line spacing, the higher the background radiation is. This in turn can diminish the spatial distribution of the etching rate along the recorded grating structure. Thus, one can assume that the initial recording of gratings with a larger line spacing is preferable for producing the surface relief grating structure being discussed. Note that this assumption is not applicable to surface relief structures composed of gratings with relatively large grating periods. The grating structure composed of the superimposed refractive index gratings exhibits other properties as well.

The appearance of "ghost" diffraction beams confirms that the surface relief profile corresponding to the total spatial distribution of electron irradiation was chemically produced in As_2S_3 film. In addition to "ghost" beams described in [11], the nontrivial "ghost" diffracted beams were created by some grating structures. In some cases, the superimposition of a subgrating with a period of about 1 μm and a grating with a beat period creates "ghost" beams. Thus, the existence of additional gratings in a grating structure was determined from analyses of the diffraction patterns.

It should be mentioned that the presence of "ghost" beams may be unwanted when the multi-beam light diffraction created by the designed grating structure is used. In this connection, it is important to determine positions of possible "ghost" beams. One can assume that the grating profile influences the intensity of "ghost" beams. Two superimposed gratings with square profiles created diffraction beams with a ratio of the intensity of a "ghost" beam to the intensity of the first-order beam of about 0.2 [11]. Such a ratio of up to 0.35 was yielded by the surface relief grating structure consisted of two superimposed gratings with non-sinusoidal profiles produced on a polymer film. The refractive index grating formed in As_2S_3 by e-beam recording has a Gaussian profile. For a small line spacing, the overlapping of lines during the recording process results in

the formation of a grating with a quasi-sinusoidal profile. Generally, the surface relief grating profile differs from the profile of the initial index grating. Nevertheless, a good correlation between these profiles can be assumed at least in the case of a short etching procedure. Thus, the surface relief grating structure probably includes gratings with quasi-Gaussian or quasi-sinusoidal profiles.

The grating structures analyzed here produced first-order "ghost" beams of low intensity. The structure composed of two gratings with Λ_1=2.0 μm and Λ_2=0.92 μm (Fig. 2) created diffraction beams with a ratio of the intensity of a "ghost" beam to the intensity of the first-order beam of about 0.15 and 0.13 for Λ_1 and Λ_2 respectively. When a structure was composed of three gratings with close periods Λ_1=1.1 μm, Λ_2=1.0 μm, and Λ_3=0.9 μm (Fig. 4), the "ghost" beams had too low intensities to be photographed. For the diffraction patterns shown in Fig. 3 and Fig. 7, the above-mentioned ratio of the intensities is about 0.1 or less than 0.1. It should be noted that the images of diffraction patterns were corrected to visualize weak "ghost" diffracted spots.

It seems, that the selection of a suitable range of the grating period is a good way to eliminate unwanted both second-order and "ghost" diffracted beams. For example, in the case of a readout laser beam of 0.633 μm, the grating structure composed of gratings with periods ranged from 0.9 to 1.6 μm will create only first-order diffracted beams spreading in the corresponding angular range.

5. Conclusions

Surface relief diffraction structures composed of superimposed unidirectional gratings created a set of distinct first-order diffracted beams. Additionally, low-intensity "ghost" diffracted beams were created. Their appearance is caused by superimposition of two gratings with different grating periods, which results both in a difference between spatial frequencies of gratings and the summation of spatial frequencies.

In the former case, the beat period between two gratings is formed. For grating structures composed of three superimposed gratings with grating periods of about 1.1, 1.0, and 0.9 μm, the order of recording of gratings influenced the diffraction efficiency of each grating The best diffraction efficiency of each grating was obtained when the primarily recorded grating was a grating with a period of 1.1 μm. Good agreement of the calculated periods of gratings corresponding to "ghost" beams with the ones determined from diffraction patterns supports the model of calculation we have used.

References

[1] T. Suhara, H. Nishihara, and J. Koyama, Jpn. J. Appl. Phys. **14**, 1079 (1975).
[2] H. Nishihara, Y. Handa, T. Suhara, and J. Koyama, Applied Optics **17** (15), 2342 (1978).
[3] T. Suhara, K. Kobayashi, H. Nishihara, J. Koyama, Applied Optics **21**(11), 1966 (1982).
[4] *O. Nordman, N. Nordman, N. Peyghambarian,* J. Appl. Phys. **84** (11), 6055 (1998).
[5] T. Suhara, H. Nishihara, IEEE Journal of Quantum Electronics **QE-22** (6), *845 (1986).*
[6] M. Vlcek, H. Jain, Journal of Optoelectronics and Advanced Materials. **8**(6), 2108 (2006).
[7] J.R. Neilson, A. Kovalskiy, M. Vlcek, H. Jain, F. Miller, Journal of Non-Crystalline Solids **353**, 1427 (2007).
[8] A. Kovalskiy, J. Cech, M. Vlcek, C. M. Waits, M. Dubey, W. R. Heffner, H. Jain J. Micro/Nanolith. MEMS MOEMS **84**, 043012-1 (2009).
[9] A. Stronski, E. Achimova, O. Paiuk, A. Meshalkin, V. Abashkin, O. Lytvyn, 2 , O. Lytvyn, S. Sergeev, A. Prisacar, G. Triduh, Nanoscale Research Letters, **11**, 39 (2016).
[10] S. A. Sergeev, A. A. Simashkevich, S. D. Shutov, Quantum Electronics **21**(10), 924 (1994).
[11] S. W. Birtwell, G. S. Galitonov, H. Morgan, N. I. Zheludev, Optics Communications **281**, 789 (2008).
[12] J.C.H. Phang and H. Ahmed, IEEE Proc., **128**, 1 (1981).